

Spin connection and boundary states in a topological insulator

V.Parente¹, P.Lucignano^{1,2}, P.Vitale^{1,3}, A.Tagliacozzo^{1,2}
and
F.Guinea⁴

¹ *Dip. Scienze Fisiche, Università di Napoli Federico II, Via Cintia, I-80126 Napoli, Italy*

² *CNR-SPIN, Monte S. Angelo-Via Cintia, I-80126, Napoli, Italy*

³ *INFN, Via Cintia, I-80126, Napoli, Italy and*

⁴ *Instituto de Ciencia de Materiales de Madrid (CSIC),
Sor Juana Inés de la Cruz 3, Madrid 28049, Spain*

We study the surface resistivity of a three-dimensional topological insulator when the boundaries exhibit a non trivial curvature. We obtain an analytical solution for a spherical topological insulator, and we show that a non trivial quantum spin connection emerges from the three dimensional band structure. We analyze the effect of the spin connection on the scattering by a bump on a flat surface. Quantum effects induced by the geometry lead to resonances when the electron wavelength is comparable to the size of the bump.

I. INTRODUCTION.

Strong Topological Insulators (TI 's) are a new class of materials with a bulk gap but surface states defined on surfaces of all orientations¹⁻⁴, making the boundaries gapless. The number of surface states at a flat surface with a given orientation is odd, and each of them shows a conical singularity, described by the two dimensional Dirac equation⁴. Localized states also exist at other lattice defects, such as screw dislocations⁵⁻⁷.

The transport features of electrons at the surfaces of TI 's is being intensively studied. The wavefunctions have an internal spinorial structure made up of two slowly varying components related by time reversal invariance. Backscattering due to smooth perturbations which preserve the time reversal symmetry is forbidden, making the transport properties of these compounds similar to those of graphene in the absence of intervalley scattering⁸. Surfaces with a finite curvature allow for scattering processes due to the existence of a non trivial metric, which has been studied in the classical limit⁹, when wavepackets are well approximated by point particles following classical trajectories.

An analysis of the electronic properties of curved surfaces of TI 's requires information about the way a non trivial metric changes the effective Dirac equation. It is well known that the Dirac equation could be written on a curved space time introducing the spin connection and the rotation of Dirac matrices¹⁰. The existence of the spin connection has been postulated in topological insulators¹¹. The emergence of the spin connection from the combination of the three dimensional electronic structure of a TI and the two dimensional metric of a boundary with intrinsic curvature has not been studied so far.

In the next section, we analyze the surface states for the simplest curved boundary with a non trivial metric, the sphere. The conservation of the angular momentum

in this geometry allows us to calculate the entire spectrum of surface states, and to show that the spin connection term is induced in the effective surface hamiltonian. We use this information in Section III to analyze the effect of the curvature in the scattering by a bump in a flat surface, a process considered in the classical limit in⁹. Related processes can be defined in graphene with topological defects¹². Technical details of the calculations are discussed in the appendices, including an analytical study of the boundary states in a cylinder, calculated numerically in¹³. The boundary of a cylinder can be considered a surface without intrinsic curvature and spin connection.

II. MODEL OF A SPHERICAL TOPOLOGICAL INSULATOR.

The surface states of model single particle hamiltonians for a TI have been studied particularly for a flat boundary¹⁴ and for an infinite cylinder boundary surface¹³. A minimal model reproducing the band structure of a TI requires four orbitals, related in pairs by the time reversal symmetry¹⁵. A further simplification includes just the linear in-momentum contributions to the hamiltonian of Ref. 15:

$$\mathcal{H} = \hat{\gamma}^0 \Delta + \hbar v_F \hat{\gamma}^i k_i \quad (\text{II.1})$$

where v_F is the Fermi velocity and the matrices $\hat{\gamma}^a$ are given in terms of Pauli matrices by $\hat{\gamma}^0 = \tau_0 \otimes \tau_z$, $\hat{\gamma}^1 = \sigma_x \otimes \tau_x$, $\hat{\gamma}^2 = -\sigma_y \otimes \tau_x$, $\hat{\gamma}^3 = \sigma_z \otimes \tau_x$. Here σ_a and τ_b denote matrices in the spin and even-odd orbital parity spaces, respectively. This hamiltonian satisfies time reversal symmetry $T = \mathcal{K} i \sigma_y \otimes \mathbb{I}_{2 \times 2}$ (here $\mathbb{I}_{2 \times 2}$ the 2×2 identity and \mathcal{K} the complex conjugation). Bulk eigenfunctions in cartesian coordinates are:

$$|\Psi_{1,\pm}\rangle = \frac{1}{N_{\pm}} \begin{pmatrix} \epsilon_{\pm}(\vec{\mathbf{k}}) + \Delta \\ \hbar v_F k_z \\ 0 \\ \hbar v_F k_- \end{pmatrix} e^{i\vec{\mathbf{k}}\cdot\vec{\mathbf{r}}}, \quad |\Psi_{2,\pm}\rangle = \frac{1}{N_{\pm}} \begin{pmatrix} 0 \\ \hbar v_F k_+ \\ \epsilon_{\pm}(\vec{\mathbf{k}}) + \Delta \\ -\hbar v_F k_z \end{pmatrix} e^{i\vec{\mathbf{k}}\cdot\vec{\mathbf{r}}} \quad (\text{II.2})$$

($k_{\pm} = k_x \pm ik_y$), where the band energies are $\epsilon_{\pm}(\vec{\mathbf{k}}) \equiv \pm\sqrt{\Delta^2 + \hbar^2 v_F^2 (k_x^2 + k_y^2 + k_z^2)}$ and N_{\pm} is the norm of the states.

Surface states appear in this model if the gap parameter, Δ , changes its sign at the boundary, so that, e.g., $\Delta > 0$ in the inside, and $\Delta < 0$ in the vacuum. The model allows also for the analytical computation of the surface bands of a cylinder¹³, as shown in Appendix A.

Later we will include also quadratic corrections to the hamiltonian in Eq.II.1 and we will show that boundary conditions need to be chosen in a different way in that case.

In order to obtain the solution of the hamiltonian II.1 onto a sphere we rephrase its eigenvalue equations into spherical coordinates. The eigenvector of energy E , $\Psi \equiv (\Psi_A, \Psi_B, \Psi_C, \Psi_D)$, satisfies the equations:

$$\begin{aligned} (E - \Delta)\Psi_A &= i \left[\cos(\theta)\partial_r - \frac{\sin(\theta)}{r}\partial_{\theta} \right] \Psi_B - ie^{-i\phi} \left[\sin(\theta)\partial_r + \frac{\cos(\theta)}{r}\partial_{\theta} - i\frac{1}{r\sin(\theta)}\partial_{\phi} \right] \Psi_D, \\ (E + \Delta)\Psi_B &= i \left[\cos(\theta)\partial_r - \frac{\sin(\theta)}{r}\partial_{\theta} \right] \Psi_A - ie^{-i\phi} \left[\sin(\theta)\partial_r + \frac{\cos(\theta)}{r}\partial_{\theta} - i\frac{1}{r\sin(\theta)}\partial_{\phi} \right] \Psi_C, \\ (E - \Delta)\Psi_C &= -ie^{i\phi} \left[\sin(\theta)\partial_r + \frac{\cos(\theta)}{r}\partial_{\theta} + i\frac{1}{r\sin(\theta)}\partial_{\phi} \right] \Psi_B - i \left[\cos(\theta)\partial_r - \frac{\sin(\theta)}{r}\partial_{\theta} \right] \Psi_D, \\ (E + \Delta)\Psi_D &= -ie^{i\phi} \left[\sin(\theta)\partial_r + \frac{\cos(\theta)}{r}\partial_{\theta} + i\frac{1}{r\sin(\theta)}\partial_{\phi} \right] \Psi_A - i \left[\cos(\theta)\partial_r - \frac{\sin(\theta)}{r}\partial_{\theta} \right] \Psi_C, \end{aligned} \quad (\text{II.3})$$

(here $\hbar = v_F = 1$), with the boundary conditions

$$\Delta(r, \theta, \phi) = \begin{cases} \Delta_{in} & r < R \\ \Delta_{out} & r > R \end{cases} \quad (\text{II.4})$$

We choose $\Delta_{in} = -\Delta_{out} = \Delta$ for simplicity, so that the exponential decay of the boundary states into the bulk near a flat surface is defined by the length scale $\Lambda = \hbar v_F / \Delta$. The angular momentum is conserved and is quantized in half integer units (see, for instance Ref. 16). Its eigenfunctions allow us to reduce the set of Eq.s(II.3) to two coupled differential equations for the radial coordinates, as discussed in Appendix B. It can be shown that the energy spectrum converges exponentially to the one of the two-dimensional Dirac equation onto a sphere:

$$\begin{aligned} E_J &= \pm \frac{\hbar v_F (J + 1/2)}{R} \times \left[1 + \mathcal{O}\left(e^{-R/\Lambda}\right) \right], \\ J &= \frac{1}{2}, \frac{3}{2}, \dots, J_{max}. \end{aligned} \quad (\text{II.5})$$

where $J_{max} \sim R/\Lambda$. The multiplicity of each level is $2J + 1$. The exponential convergence of the energy levels to the asymptotic value in eq. II.5 is shown in Fig. 1. This type of convergence implies that the effective hamiltonian describing the surface modes does not admit an expansion on higher order derivatives, of the type $\Delta(\Lambda\partial_i)^n$.

The study of the hamiltonian in eq. II.1 can be extended in a straightforward way to the case when $\Delta_{out} \neq \Delta_{in}$, although it becomes cumbersome to obtain analytical expansions in the limit $R \rightarrow \infty$. The numerical solution, obtained by generalizing the analysis of Appendix B, shows an agreement with the spectrum in Eq. II.5 of the same accuracy as those reported in Fig. 1.

As quadratic terms do not break the spherical symmetry, they can be safely added to Eq. II.1, by the simple substitution $\Delta \rightarrow \Delta + \alpha(k_x^2 + k_y^2 + k_z^2)$, where α is a constant. Hence the angular part of the wavefunctions remains unchanged while its radial part satisfies second order coupled equations, in place of those in Eq. II.3. For each value of the energy, E , we find evanescent waves with two different decay lengths, $\Lambda_1(E)$ and $\Lambda_2(E)$, which are given by the roots of a fourth order polynomial. The boundary conditions need to be replaced. The simplest boundary condition compatible with the new second order equations is $\Psi_A(R) = \Psi_B(R) = \Psi_C(R) = \Psi_D(R) = 0$ ¹⁴. By solving numerically these boundary conditions, we find again an agreement with eq. II.5 similar to that shown in Fig. 1. Results are shown in Fig. 2.

We conclude that the boundary states on a spherical TI satisfy the Dirac equation on the surface of the sphere. The spin connection, related to the intrinsic cur-

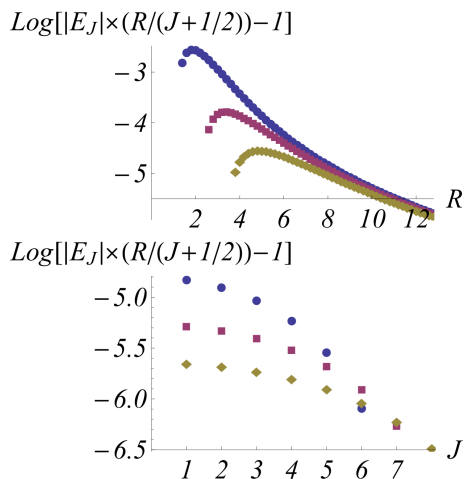


FIG. 1: (Color online). Dependence of the surface energy levels on angular momentum, J , and radius, R . The deviation from the result for the two dimensional Dirac equation on a sphere, see eq. II.5 is plotted. Top: Dependence on R . From top to bottom, $J = 1, 2, 3$. Bottom: Dependence on J . From top to bottom, $R = 8, 10, 12$. In all cases, $v_F = 1$ and $\Delta = 1$.

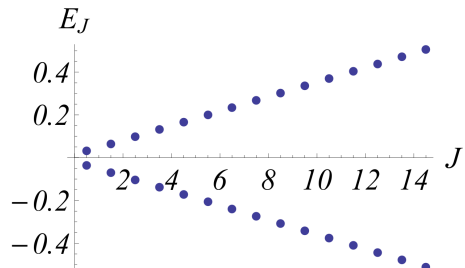


FIG. 2: (Color online). Energy levels of a spherical topological insulator of radius $R = 30$ with a quadratic dispersion relation, obtained by the replacement $\Delta \rightarrow \Delta + \alpha(k_x^2 + k_y^2 + k_z^2)$ in eq. II.1. Other parameters are $\Delta = 1$ and $v_F = 1$. The boundary conditions are $\Psi_A(R) = \Psi_B(R) = \Psi_C(R) = \Psi_D(R) = 0$.

vature of the metric, clearly emerges at the boundaries of a TI. More generally, the boundary states satisfy the Dirac equation on a curved space-time¹⁰

$$\gamma^\mu (\partial_\mu + \Gamma_\mu) \Psi = 0 . \quad (\text{II.6})$$

Here $\gamma^\mu = e_a^\mu \gamma^a$ (with $\gamma^{a=0} = -i\sigma^z, \gamma^{a=1} = \sigma^y$ and $\gamma^{a=2} = -\sigma^x$) are the rotated Dirac matrices, satisfying the generalization of the flat algebra

$$\{\gamma^\mu, \gamma^\nu\} = 2g^{\mu\nu} . \quad (\text{II.7})$$

The Minkowski metric η_{ab} has been replaced by the curved one $g_{\mu\nu} = \eta_{ab} e^a_\mu e^b_\nu$. The tetrads e^a_μ are the elements of the Jacobian matrix of the transformation from the coordinates x^μ , defined on the whole manifold,

to a local inertial frame:

$$e^a_\mu = \frac{\partial x^a}{\partial x^\mu} . \quad (\text{II.8})$$

Γ_μ is the spin connection $\frac{i}{2} \Gamma_\mu^{ab} \Sigma_{ab}$ where $\Sigma_{ab} = i/2[\gamma_a, \gamma_b]$ are the generators of the spinorial representation of the Lorentz group, and the connection coefficients Γ_μ^{ab} are given by $\Gamma_\mu^{ab} = e^a_\nu \nabla_\mu e^{b\nu}$.

III. SCATTERING OFF A GAUSSIAN BUMP

A. Unrelaxed lattice

We now derive the resistivity for electrons propagating at the flat boundary surface of a TI, when they are scattered off a gaussian bump of height $z(|\vec{r}|) = h e^{-r^2/\ell^2}$. The Boltzmann relaxation-time approximation can be used ($\nu(0) = k_F/(\pi\hbar v_F)$ is the density of states at the Fermi level for both spins):

$$\rho(k_F) = \frac{2}{e^2 v_F^2 \nu(0)} \frac{1}{\tau(k_F)} , \quad (\text{III.9})$$

where the usual definition of the total relaxation rate is

$$\frac{1}{\tau(k_F)} = \frac{2\pi}{\hbar} \nu(0) \int_0^{2\pi} d\theta (1 - \hat{k} \cdot \hat{k}') |\langle k | t^{eff} | k' \rangle|^2 . \quad (\text{III.10})$$

Here $\langle k | t^{eff} | k' \rangle$ is the matrix element of the t -matrix, which depends on the energy and on the scattering angle θ between the incoming and outgoing wave.

Since the metric induced on the manifold by the bump is axially symmetric, it is convenient to rewrite the two dimensional Dirac equation in flat space time in cylindrical coordinates:

$$-i\hbar v_F \left(\sigma^r \partial_r + \sigma^\theta \frac{1}{r} \partial_\theta \right) \Psi = E \Psi . \quad (\text{III.11})$$

Here the matrices $\sigma^{r,\theta}$ are $\sigma^r = \cos \theta \sigma^x + \sin \theta \sigma^y$ and $\sigma^\theta = -\sin \theta \sigma^x + \cos \theta \sigma^y$.

Given the metric¹⁷

$$g_{\mu\nu} = \begin{pmatrix} -1 & 0 & 0 \\ 0 & 1 + f(r) & 0 \\ 0 & 0 & r^2 \end{pmatrix} , \quad (\text{III.12})$$

where $f(r) = (dz(r)/dr)^2$, we rewrite Eq.(II.6) and, as shown in Appendix C, the spin connection Γ_μ can be embodied in the wavefunction as a real prefactor $\Psi = \Phi \exp \int_r^{+\infty} dr' A_\theta(r')$, where $A_\theta(r) = \frac{1}{2r} (\sqrt{1 + f(r)} - 1)$. The spinor Φ satisfies the equation

$$-i \left[\frac{\sigma^r}{\sqrt{1 + f(r)}} \frac{\partial}{\partial r} + \sigma^\theta \frac{1}{r} \frac{\partial}{\partial \theta} \right] \Phi = s k \Phi . \quad (\text{III.13})$$

where $s = +(-)$ for particles (holes) and $E = \hbar v_F k$. The

real prefactor can be interpreted as the origin of charge puddles accumulating at the bump. Eq. (III.13) describes an unrelaxed lattice. Relaxation of the structure, besides adding an effective gauge potential, may further change the spin connection. As elastic deformations do not add any curvature, the change only implies a trivial holonomy on the wave function. This is a way of restating the Saint Venant conditions for the two-dimensional case. Changes in the Dirac Equations are well localized in space close to the bump, hence a scattering picture can be fruitfully adopted here. We will focus on the par-

ticle sector of the theory, and assume that the incoming k -vector is in the direction of the polar axis ($\theta = 0$). The eigenfunctions can be expressed as superposition of angular momentum m eigenstates:

$$\Phi_m(r, \theta) = \begin{pmatrix} u_m(r) \\ i v_m(r) e^{i\theta} \end{pmatrix} e^{im\theta} . \quad (\text{III.14})$$

The Born approximation is worked out, to lowest order, in Appendix C. Using an asymptotic expansion of the wavefunctions given in Eq.(D.9), we have:

$$\frac{1}{\tau(\vec{k}_F)} = \frac{n_b v_F}{k_F} \times \sum_m [\sin^2 \delta_m - \cos(\delta_{m+1} - \delta_{m-1}) \sin \delta_{m+1} \sin \delta_{m+1}] \quad (\text{III.15})$$

where the phase shifts δ_m for the m^{th} component of the wavefunction are reported in appendix C and n_b is the concentration of bumps.

At low incoming electron energy, it turns out that the terms with $m = 0, \pm 1, \pm 2$ are $\mathcal{O}[(k\ell)^4]$ and when choosing $4\pi^2 h^2 / \ell^2 \sim 1$, they sum up to $\mathcal{S} \approx 0.733$. The terms with $m = \pm 3$ are $\mathcal{O}[(k\ell)^8]$, while the terms $m = \pm 4$ are $\mathcal{O}[(k\ell)^{12}]$ (see Appendix C).

Eventually, the resistivity for independent point like defects, when the carrier density is low, (i.e. low incoming energy) is:

$$\rho(k_F) \sim \frac{2h}{e^2} n_b \pi \ell^2 \left\{ \mathcal{S} \left(\frac{h}{\ell} \right) (k_F \ell)^2 + \mathcal{O}[(k_F \ell)^4] \right\} . \quad (\text{III.16})$$

$\mathcal{S}(h/\ell)$ is a numerical prefactor which depends on the strength of the perturbation parametrized by h/ℓ . The plot of the resistivity *vs* energy in dimensionless units, $k_F \ell$, for various values of h/ℓ is shown in Fig. 3. The leading term is proportional to the density of carriers n .

It has been proven recently that the classical limit for large incoming energy (i.e. relatively high densities n) corresponds to an energy independent $v_F \tau(k_F)^9$. This implies that, according to Eq.(III.9), $\rho \propto h/(e^2 k_F) \sim 1/\sqrt{n}$, in this limit. We derive the same conclusion with a careful analysis of the sum in Eq.(III.15) at $k\ell \gg 1$. Classically, angular momentum conservation in the scattering implies that $m \sim kb$. Here b is the impact parameter measured from the center of the bump in the direction orthogonal to \vec{k} . By asymptotically expanding the Bessel functions appearing in the phase shifts, it turns out that there is a collection of terms contributing to the sum, which are roughly independent of m , as long as $k\ell \gg m$. For these m values, $\tan \delta_m$ is of the form:

$$\tan \delta_m \approx \pi \left(\frac{h}{\ell} \right)^2 \frac{k\ell}{2} \left[\sqrt{\frac{\pi}{2}} - (-1)^m \frac{2}{(k\ell)^3} \right] \quad (\text{III.17})$$

All other terms scale for $m \gg k\ell$ as

$$\sqrt{\frac{m}{2}} \left(\frac{k\ell}{2} \right)^{2(m+1)} \frac{1}{(2m-1)!!} \quad (\text{III.18})$$

and therefore they rapidly converge to zero.

We conclude that in the semiclassical limit $k\ell \gg 1$ a factor k_F comes from the relevant terms in the sum of Eq.(III.15), which are all of the same order. This factor cancels with the k_F appearing in the denominator, so that the result for $v_F \tau(k_F)$ is independent of k_F . This is in fact found numerically. In Fig. 3 we see that the conductivity $\sim \rho^{-1}$ grows linearly at large $k_F \ell$ and has a minimum in the neighborhood of $k_F \ell \sim 1$. In Appendix D we report a simple argument based on a saddle point approximation of the \sum_m which qualitatively recovers the classical limiting result for large $k_F \ell$, derived in Ref. 9. In Fig. 3 it is shown a significant increase of the cross section of the bump for $k_F \ell \sim 1$ and $h/\ell \gtrsim 0.2$. This increase is due to quantum resonances induced by the non trivial spin connection.

IV. DISCUSSION.

We have shown in Section II how the two dimensional Dirac equation in curved space emerges at the simplest boundary with non trivial metric, the surface of a sphere. The metric enters through the spin connection, which reflects the properties of the internal spin under parallel transport along the surface¹⁰. The spin connection reflects a quantum feature of the electrons, and cannot be inferred from solely classical arguments. The spin connection leads to a finite Berry phase when the electron is transported around a closed geodesic. A manifestation of this effect is the quantization of the total angular momentum in half integer units.

The model that we have studied leads to simple analytical expressions of the energies and wavefunctions of

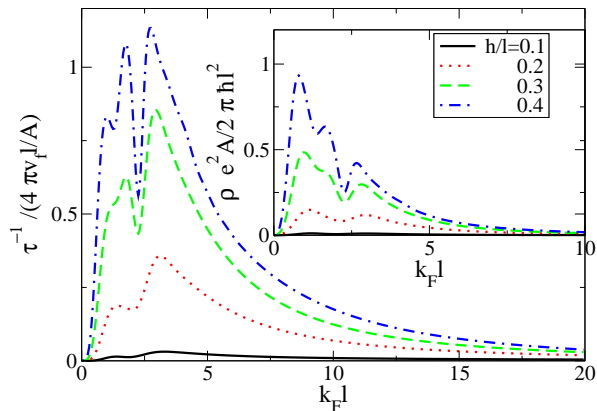


FIG. 3: (Color on-line) Main Panel: inverse scattering time as a function of $k_F l$ for different values of the aspect ratio of the bump h/l . Inset: the resistivity due to scattering off a bump on the surface of a topological insulator, in units $\rho \cdot e^2 A / (2\pi \hbar l^2)$ vs. dimensionless energy $k l$, at different ratios h/l .

the boundary states. They can be used as a zeroth approximation to situations close to spherical symmetry, or where an isotropic electronic structure can be obtained by rescaling a length. We find that the corrections to the two dimensional Dirac equation depend exponentially on $R/\Lambda \equiv R\Delta/\hbar v_F$ ¹⁸.

The model describes external surfaces of mesoscopic crystals and internal voids in bulk systems. In the case of a small void, we find that two doublets at a finite distance of the Dirac energy appear for radii $R \gtrsim 2/\Lambda$. These voids will act as molecules embedded into the bulk material. The interaction energy of electrons localized inside the voids scales as the level separation, $E_{int} \approx e^2/(\epsilon R)$, where ϵ is the dielectric constant of the topological insulator. At temperatures below this scale, voids with an odd number of electrons will give rise to magnetic moments. The RKKY interaction between moments at different vacancies should decay exponentially, $J_{RKKY}(\vec{r} - \vec{r}') \sim e^{-|\vec{r} - \vec{r}'|/\Lambda}$. Hence, small vacancies might give rise to a paramagnetic susceptibility in topological insulators. If they are within a distance $d \sim \Lambda$ from the surface, these local moments will hybridize with the surface states, leading to the Kondo effect^{19,20}.

We have analyzed the scattering of Dirac fermions by surface corrugations which induce a non trivial curvature in the quantum limit, $k_F l \lesssim 1$. We find that the resistivity due to a finite concentration of bumps, n_b , vanishes as k_F^2 for small k_F , due to a combination of a density of states factor, which goes as k_F , and a scattering time which increases as k_F^{-3} . By comparison, the scattering time in the classical regime⁹ ($k_F l \rightarrow \infty$) is independent of k_F , and $\rho \sim k_F^{-1}$. The wave nature of the quasiparticles allow them to diffract around the bump, making it effectively transparent for long wavelengths, $k_F l \ll 1$. The non trivial curvature induces quantum resonances for $k_F l \sim 1$ and an aspect ratio $h/l \gtrsim 0.2$.

Acknowledgments

We acknowledge important discussions with A. Akhmerov, R. Egger and M. A. H. Vozmediano. We acknowledge financial support from MIDAS (Macroscopic Interference Devices for Atomic and Solid State Physics) and from MAMA (Multifunctioned Advanced Materials and nanoscale phenomena) F.G. is supported by MICINN (Spain), Grants FIS2008-00124 and CONSOLIDER CSD2007-00010.

Appendix A: Boundary states at cylinder surface

In the following appendixes we will use $\hbar = v_F = 1$, except in main results. Let us start from the $\vec{k} \cdot \vec{p}$ model Hamiltonian of Eq.(II.1):

$$H[\vec{r}] = \begin{pmatrix} \Delta & i\partial_z & 0 & i(\partial_x + i\partial_y) \\ i\partial_z & -\Delta & i(\partial_x + i\partial_y) & 0 \\ 0 & i(\partial_x - i\partial_y) & \Delta & -i\partial_z \\ i(\partial_x - i\partial_y) & 0 & -i\partial_z & -\Delta \end{pmatrix}. \quad (\text{A.1})$$

To find surface states in this approximation is enough to match the solutions of the Schrödinger equation at the surface of the cylinder. The gap Δ should change its sign between in and out of the surface. We rewrite the eigenvalue problem in cylindrical coordinates for the 4-component spinor $(\Psi_A, \Psi_B, \Psi_C, \Psi_D)$:

$$\begin{aligned}
(E - \Delta) \Psi_A(\vec{r}) &= i \frac{\partial}{\partial z} \Psi_B(\vec{r}) + e^{i\theta} \left(i \frac{\partial}{\partial r} - \frac{1}{r} \frac{\partial}{\partial \theta} \right) \Psi_D(\vec{r}) \\
(E + \Delta) \Psi_B(\vec{r}) &= i \frac{\partial}{\partial z} \Psi_A(\vec{r}) + e^{i\theta} \left(i \frac{\partial}{\partial r} - \frac{1}{r} \frac{\partial}{\partial \theta} \right) \Psi_C(\vec{r}) \\
(E - \Delta) \Psi_C(\vec{r}) &= e^{-i\theta} \left(i \frac{\partial}{\partial r} + \frac{1}{r} \frac{\partial}{\partial \theta} \right) \Psi_B(\vec{r}) - i \frac{\partial}{\partial z} \Psi_D(\vec{r}) \\
(E + \Delta) \Psi_D(\vec{r}) &= e^{-i\theta} \left(i \frac{\partial}{\partial r} + \frac{1}{r} \frac{\partial}{\partial \theta} \right) \Psi_A(\vec{r}) - i \frac{\partial}{\partial z} \Psi_C(\vec{r})
\end{aligned} \tag{A.2}$$

(in the following k is in the \hat{z} direction, which is the axis of the infinite cylinder. Inside the cylinder, the wavefunctions which are mostly localized close to the surface involve the modified Bessel functions $I_n(\kappa r)$ with integer n . They diverge exponentially at infinity but are finite for $r \rightarrow 0$. The two eigenfunctions at fixed energy E are (κ is unknown for the moment):

$$|E, 1_{<}\rangle = \frac{1}{N} \begin{pmatrix} (E + \Delta) I_n(\kappa r) \\ k I_n(\kappa r) \\ 0 \\ i\kappa I_{n+1}(\kappa r) e^{-i\theta} \end{pmatrix} e^{-in\theta} e^{-ikz}, \quad |E, 2_{<}\rangle = \frac{1}{N} \begin{pmatrix} i\kappa I_n(\kappa r) e^{i\theta} \\ 0 \\ -k I_{n+1}(\kappa r) \\ (E - \Delta) I_{n+1}(\kappa r) \end{pmatrix} e^{-i(n+1)\theta} e^{-ikz}. \tag{A.3}$$

The energies of these states are $E = \pm \sqrt{\Delta^2 + k^2 - \kappa^2}$. Outside the cylinder, the functions $K_n(\kappa r)$ replace the $I_n(\kappa r)$, as the former decay exponentially for $\kappa r \rightarrow \infty$ and $\Delta \rightarrow -\Delta$. The eigenfunctions are:

$$|E, 1_{>}\rangle = \frac{1}{N} \begin{pmatrix} (E - \Delta) K_n(\kappa r) \\ k K_n(\kappa r) \\ 0 \\ -i\kappa K_{n+1}(\kappa r) e^{-i\theta} \end{pmatrix} e^{-in\theta} e^{-ikz}, \quad |E, 2_{>}\rangle = \frac{1}{N} \begin{pmatrix} -i\kappa K_n(\kappa r) e^{i\theta} \\ 0 \\ -k K_{n+1}(\kappa r) \\ (E + \Delta) K_{n+1}(\kappa r) \end{pmatrix} e^{-i(n+1)\theta} e^{-ikz}. \tag{A.4}$$

The eigenvalues are again those of Eq.(A.3)

The two wavefunctions inside the cylinder should be matched to the two outside for each value of n . The

matching conditions at R , the radius of the cylinder, lead to

$$\text{Det} \begin{vmatrix} i\kappa I_n(\kappa R) & (E + \Delta) I_n(\kappa R) & -i\kappa K_n(\kappa R) & (E - \Delta) K_n(\kappa R) \\ 0 & k I_n(\kappa R) & 0 & k K_n(\kappa R) \\ -k I_{n+1}(\kappa R) & 0 & -k K_{n+1}(\kappa R) & 0 \\ (E - \Delta) I_{n+1}(\kappa R) & i\kappa I_{n+1}(\kappa R) & (E + \Delta) K_{n+1}(\kappa R) & -i\kappa K_{n+1}(\kappa R) \end{vmatrix} = 0. \tag{A.5}$$

The vanishing of the determinant implies:

$$[I_n^2 K_{n+1}^2 + K_n^2 I_{n+1}^2] \kappa^2 + (2\kappa^2 - 4\Delta^2) I_n I_{n+1} K_n K_{n+1} = 0. \tag{A.6}$$

The presence of products of the Bessel functions I_n and K_n assures that, in the limit of $\kappa R \gg 1$, there is just an inverse powerlaw dependence of the secular problem on κR . and Eq.(A.6) becomes:

$$\kappa^2 = \Delta^2 \left[1 - \frac{(n + 1/2)^2}{\Delta^2 R^2} \right]. \tag{A.7}$$

Hence, the energy of the states is, according to Eq.(A.8)

$$E = \pm \hbar v_F \sqrt{k^2 + \frac{(n + 1/2)^2}{R^2}} + \mathcal{O} \left(\frac{\hbar v_F^2}{\Delta^2 R^2} \right) \quad R \gg \frac{\hbar v_F}{\Delta} \tag{A.8}$$

This result is in complete agreement with Eq.5 of Ref. 13. Let us now consider the opposite limit $\kappa R \ll 1$.

Expansion gives, up to second order in $1/\kappa R$:

$$\kappa^2 \left\{ 2n(n+1) \left[1 + \frac{1}{16 n^2(n+1)^2} \right] + \frac{1}{2} \right\} = \Delta^2 . \quad (\text{A.9})$$

The energy reads in this limit:

$$E_n(k) \approx \pm \Delta \sqrt{1 - 1/\left(2n(n+1) \left[1 + \frac{1}{16 n^2(n+1)^2} \right] + \frac{1}{2} \right)} + \left(\frac{\hbar v_F k_z}{\Delta} \right)^2 + \mathcal{O} \left(\frac{\hbar \Delta R}{v_F} \right) \quad \text{for } R \ll \hbar v_F / \Delta . \quad (\text{A.10})$$

Appendix B: Angular momentum eigenstates

Generalized angular momentum operators J can be defined as usual as the sum of spin and orbital angular momentum. It can be shown that the Hamiltonian in eq. II.3 commutes with J^2, J_z therefore its eigenstates can be labeled by $|j, m\rangle$ with $\mathbf{J}^2|j, m\rangle = j(j+1)|j, m\rangle$

and $J_z|j, m\rangle = m|j, m\rangle$. In order to obtain single valued eigenfunctions, the values of J and J_z must be half integers. As usual by using $J^+|j, j\rangle = 0$ and $J^-|j, m\rangle \propto |j, m-1\rangle$ we can explicitly construct the wavefunctions of the different states $|j, m\rangle$. The Hamiltonian eigenfunction can be thus expanded onto the the lowest angular momenta states:

$$\begin{aligned} \left| \frac{1}{2}, \frac{1}{2} \right\rangle &= A \begin{pmatrix} -\cos(\theta) \\ 0 \\ \sin(\theta)e^{i\phi} \\ 0 \end{pmatrix} + B \begin{pmatrix} 0 \\ -\cos(\theta) \\ 0 \\ \sin(\theta)e^{i\phi} \end{pmatrix} + C \begin{pmatrix} 1 \\ 0 \\ 0 \\ 0 \end{pmatrix} + D \begin{pmatrix} 0 \\ 1 \\ 0 \\ \theta \end{pmatrix} \\ \left| \frac{1}{2}, -\frac{1}{2} \right\rangle &= A \begin{pmatrix} \sin(\theta)e^{-i\phi} \\ 0 \\ \cos(\phi) \\ 0 \end{pmatrix} + B \begin{pmatrix} 0 \\ \sin(\theta)e^{-i\phi} \\ 0 \\ \cos(\phi) \end{pmatrix} + C \begin{pmatrix} 0 \\ 0 \\ 1 \\ 0 \end{pmatrix} + D \begin{pmatrix} 0 \\ 0 \\ 0 \\ 1 \end{pmatrix} \\ \left| \frac{3}{2}, \frac{3}{2} \right\rangle &= A \begin{pmatrix} -\sin(\theta)\cos(\theta)e^{i\phi} \\ 0 \\ \sin^2(\theta)e^{2i\phi} \\ 0 \end{pmatrix} + B \begin{pmatrix} 0 \\ -\sin(\theta)\cos(\theta)e^{i\phi} \\ 0 \\ \sin^2(\theta)e^{2i\phi} \end{pmatrix} + C \begin{pmatrix} \sin(\theta)e^{i\phi} \\ 0 \\ 0 \\ 0 \end{pmatrix} + D \begin{pmatrix} 0 \\ \sin(\theta)e^{i\phi} \\ 0 \\ 0 \end{pmatrix} \\ \left| \frac{3}{2}, \frac{1}{2} \right\rangle &= A \begin{pmatrix} -2\cos^2(\theta) + \sin^2(\theta) \\ 0 \\ 3\sin(\theta)\cos(\theta)e^{i\phi} \\ 0 \end{pmatrix} + B \begin{pmatrix} 0 \\ -2\cos^2(\theta) + \sin^2(\theta) \\ 0 \\ 3\sin(\theta)\cos(\theta)e^{i\phi} \end{pmatrix} + C \begin{pmatrix} 2\cos(\theta) \\ 0 \\ \sin(\theta)e^{i\phi} \\ 0 \end{pmatrix} + D \begin{pmatrix} 0 \\ 2\cos(\theta) \\ 0 \\ \sin(\theta)e^{i\phi} \end{pmatrix} \quad (\text{B.1}) \end{aligned}$$

where the states $|3/2, -1/2\rangle, |3/2, -3/2\rangle$ are not explicitly exhibited, here.

form:

Appendix C: Spherical boundary states and energy spectrum

It can be shown that boundary states in the spherical case for $j = m = n - 1/2$ ($n > 0$) have the following

$$\left\langle r, \theta, \phi \left| J - \frac{1}{2}, J_z - \frac{1}{2} \right. \right\rangle = f_1^\mp(r) \begin{pmatrix} 0 \\ -\cos\theta \sin^{n-1}\theta e^{i(n-1)\phi} \\ 0 \\ \sin^n\theta e^{in\phi} \end{pmatrix} + f_2^\mp(r) \begin{pmatrix} \sin^{n-1}\theta e^{i(n-1)\phi} \\ 0 \\ 0 \\ 0 \end{pmatrix}. \quad (\text{C.1})$$

Here $f^-(r)$ and $f^+(r)$ are radial functions localized at the boundary for $r < R$ and $r > R$, respectively, and they satisfy the equations:

$$\begin{aligned} (E \mp \Delta) f_2^\mp &= -i\partial_r f_1^\mp - \frac{i}{r}(n+1)f_1^\mp, \\ (E \pm \Delta) f_1^\mp &= -i\partial_r f_2^\mp + \frac{i}{r}(n-1)f_2^\mp. \end{aligned} \quad (\text{C.2})$$

The system can be decoupled in a pair of Bessel equations

$$\begin{aligned} \frac{d^2}{dr^2} f_1^\pm + \frac{2}{r} \frac{d}{dr} f_1^\pm - \left[(\Delta^2 - E^2) + \frac{n(n+1)}{r^2} \right] f_1^\pm &= 0, \\ \frac{d^2}{dr^2} f_2^\pm + \frac{2}{r} \frac{d}{dr} f_2^\pm - \left[(\Delta^2 - E^2) + \frac{n(n-1)}{r^2} \right] f_2^\pm &= 0, \end{aligned} \quad (\text{C.3})$$

whose solutions are:

$$\begin{aligned} if \ r < R & \quad \begin{cases} f_1^-(r) = -i\frac{\Delta-E}{\kappa} C^- i_n(\kappa r) \\ f_2^-(r) = C^- i_{n-1}(\kappa r) \end{cases} \\ if \ r > R & \quad \begin{cases} f_1^+(r) = -iC^+ \frac{\Delta+E}{\kappa} k_n(\kappa r) \\ f_2^+(r) = C^+ k_{n-1}(\kappa r) \end{cases} \end{aligned} \quad (\text{C.4})$$

where i_n, k_n are the modified spherical Bessel functions:

$$i_n(x) \equiv \sqrt{\frac{\pi}{2x}} I_{n+\frac{1}{2}}(x), \quad k_n(x) \equiv \sqrt{\frac{\pi}{2x}} K_{n+\frac{1}{2}}(x). \quad (\text{C.5})$$

The matching conditions can be written using Eq. (C.4)

$$\begin{cases} -iC^- (\Delta - E) i_n(\kappa R) = -iC^+ (\Delta + E) k_n(\kappa R), \\ C^- i_{n-1}(\kappa R) = C^+ k_{n-1}(\kappa R), \end{cases} \quad (\text{C.6})$$

which give rise to an implicit equation for the eigenenergies of the system:

$$\frac{\Delta - E}{\Delta + E} = -\frac{k_n(\kappa R) i_{n-1}(\kappa R)}{i_n(\kappa R) k_{n-1}(\kappa R)}. \quad (\text{C.7})$$

This equation, in the limit $\Delta R \rightarrow \infty$, gives the admissible values of the energy:

$$E_n = \pm n \frac{\hbar v_F}{R}, \quad n = 1, \dots, n_{max} \quad (\text{C.8})$$

which is reported in Sec. II.

Appendix D: Derivation of the elastic t -matrix for scattering off a gaussian bump

We derive the elastic t -matrix when a localized deformation is present on the surface of a TI. As in¹⁷ we consider a two-dimensional spatial sheet modeled on a two-dimensional axial symmetric manifold with a single gaussian bump. The axial symmetric gaussian surface may be represented in Minkowski space-time by the function $\phi = (t, x, y, h(r))$ with $r^2 = x^2 + y^2$. From Eqs. (III.12), we may read the tetrads

$$\begin{aligned} e_x^1 &= \frac{\cos\theta}{\sqrt{1+f(r)}}, & e_y^1 &= \frac{\sin\theta}{\sqrt{1+f(r)}}, \\ e_x^2 &= -\frac{\sin\theta}{r}, & e_y^2 &= \frac{\cos\theta}{r}. \end{aligned} \quad (\text{D.1})$$

The Dirac equation on a radially symmetric manifold is

$$-i \left[\frac{\sigma^r}{\sqrt{1+f(r)}} \partial_r + \sigma^\theta \left(\frac{1}{r} \partial_\theta + \frac{i}{2r} \left(1 - \frac{1}{\sqrt{1+f(r)}} \right) \sigma^z \right) \right] \Psi = E \Psi, \quad (\text{D.2})$$

The gauge potential in (D.2) is the spin connection

$$\Gamma_\mu = \frac{i}{2} \left(1 - \frac{1}{\sqrt{1+f(r)}} \right) \sigma^z \delta_{\mu 2}. \quad (\text{D.3})$$

We pose $\Psi = \Phi \exp \int_r^{+\infty} dr' A_\theta(r')$ with A_θ is the spin connection above. The m component of the spinor Φ has

the form (m is the angular momentum integer):

$$\Phi_m(r, \theta | \vec{k}, s) = \begin{pmatrix} u_{sm}(r) \\ is v_{sm}(r) e^{i\theta} \end{pmatrix} e^{im(\theta - \theta_k)} \quad (\text{D.4})$$

where θ_k is the angle that the direction of the \vec{k} vector of the incoming wave forms with the polar axis. Substitut-

ing (D.4) in the Dirac eq.(III.13) and dropping the labels sm , we find that the functions $u(r), v(r)$ have to satisfy the following equations:

$$\begin{aligned} \frac{1}{\sqrt{1+f}} \frac{d^2 u(r)}{dr^2} + \frac{1}{r} \frac{du(r)}{dr} + \left(\frac{d}{dr} \frac{1}{\sqrt{1+f}} \right) \frac{du(r)}{dr} - \frac{m^2}{r^2} \sqrt{1+f} u(r) + k^2 u(r) &= 0, \\ \frac{1}{\sqrt{1+f}} \frac{d^2 v(r)}{dr^2} + \frac{1}{r} \frac{dv(r)}{dr} + \left(\frac{d}{dr} \frac{1}{\sqrt{1+f}} \right) \frac{dv(r)}{dr} - \frac{(m+1)^2}{r^2} \sqrt{1+f} v(r) + k^2 v(r) &= 0. \end{aligned} \quad (\text{D.5})$$

Due to the symmetry of the problem is suitable to expand the Green's function for the flat space-time problem in polar coordinates

$$G(z, z') = \frac{1}{2\pi} \sum_{m=-\infty}^{+\infty} e^{im(\theta - \theta')} g_m(r, r'). \quad (\text{D.6})$$

The Green function displaying the correct jump of the derivative at $r = r'$ is:

$$g_m(x, x') = 2\pi^2 J_m(x_<) Y_m(x_>) . \quad (\text{D.7})$$

Here $r_<(r_>)$ is the smaller (larger) of the two arguments r, r' . We now specialize the shape of the bump $h(r)$ to

be the gaussian bump $z(|\vec{r}'|)$ defined in sec. III.A. This implies that $f(r) = (4h^2 r^2 / \ell^4) e^{-2(r/\ell)^2}$. We assume that the ratio h/ℓ is small, so that we can expand Eq.s (D.5) by retaining just the lowest power of h/ℓ . By comparison with the system for the flat space (i.e. $f(r) = 0$), we define the perturbative potential :

$$\frac{h^2}{\ell^2} V_m(r) = \frac{2h^2}{\ell^4} r^2 e^{-2r^2/\ell^2} \left[\frac{d^2}{dr^2} + \left(\frac{4}{r} - \frac{8r}{\ell^2} \right) \frac{d}{dr} - \frac{m^2}{r^2} \right]. \quad (\text{D.8})$$

In the Born approximation, the Dyson equation for e.g. u_{km} reads:

$$\begin{aligned} u_{km}(r) &= J_m(kr) + \frac{h^2}{\ell^2} \int_0^\infty dr' r' g_m(r, r') V_m(r') J_m(kr') \\ &= J_m(kr) + \frac{2h^2}{\ell^4} \int_0^\infty dr' g_m(r, r') r'^3 e^{-2r'^2/\ell^2} \left\{ k^2 + \left(\frac{3}{r'} - \frac{8r'}{\ell^2} \right) \frac{d}{dr'} \right\} J_m(kr') \end{aligned} \quad (\text{D.9})$$

We have used the fact that J_m solves the Bessel differential equation to simplify the action of V_m on J_m itself.

By defining :

$$\tan \delta_m = \frac{4\pi^2 k^2 h^2}{\ell^4} \int_0^\infty dr' J_m(kr') r'^3 e^{-2r'^2/\ell^2} \left\{ 1 + \frac{1}{k^2} \left(\frac{3}{r'} - \frac{8r'}{\ell^2} \right) \frac{d}{dr'} \right\} J_m(kr') , \quad (\text{D.10})$$

the scattering state for $r/\ell \rightarrow \infty$ takes the form $u_{km}(r) \sim J_m(kr) + \tan \delta_m Y_m(kr)$. By exploiting the symmetry of the Dirac massless equation with respect to replacements

$u \leftrightarrow v, m \leftrightarrow -m-1$, it is easy to see, that the sums which include δ_m , for all m , are equal. Therefore, our result is valid for both components of the spinor solution given by

Eq.(III.14).

The integrals of Eq.(D.10) can be evaluated analytically. The asymptotic expansion of the Bessel functions

implies that, far from the bump ($r/\ell \rightarrow \infty$), the outgoing wave takes the form:

$$u_{km}(r) \sim_{r/\ell \rightarrow \infty} \frac{1}{\sqrt{1 + \tan^2 \delta_m}} \cos \chi_m + \frac{\tan \delta_m}{\sqrt{1 + \tan^2 \delta_m}} \sin \chi_m \equiv \cos(\chi_m + \delta_m) \quad \chi_m = kr - \frac{m\pi}{2} - \frac{\pi}{4}.$$

We now evaluate the t - matrix element for a scattering event, in which an incoming wave with wavevector \vec{k} is

scattered elastically by the gaussian bump and a plane wave of wavevector \vec{p} emerges. The t -matrix element is:

$$\langle p | t(\vec{k}) | k \rangle = \left[1 + e^{-i(\theta_p - \theta_k)} \right] \sqrt{\frac{2}{\pi k R^2}} e^{i\pi/4} \frac{1}{R} \int_0^R dr e^{\frac{k^2}{\ell^4} \int_r^R dr' r'^2 e^{-2(r'/\ell)^2}} \sum_m [e^{2i\delta_m} - 1] e^{-im(\theta_p - \theta_k)}.$$

The space integral arises from the exponential prefactor of Ψ defined before Eq.(III.13). To evaluate the relaxation time formula of Eq.(III.15) we first perform the integral over the angle θ_p of the square modulus of the angle dependent exponentials in the sums. The integral is non vanishing only for $m - m' = \pm 2, 0$. By rearranging the sums then eq. (III.15) is obtained.

saddle point approximation to the resulting integral²¹:

$$\sum_m e^{i(2\delta_m + m\theta)} \approx e^{i(2\delta_{m_0} + m_0\theta)} \times \int dm e^{i \frac{d^2 \delta}{dm^2} \Big|_0 (m - m_0)^2}. \quad (\text{E.3})$$

Here m_0 is the stationary point, which solves the saddle point equation:

$$\frac{d\delta_m}{dm} \Big|_{m_0} - \frac{\theta}{2} = 0. \quad (\text{E.4})$$

Derivation of this equation, once more, provides a relation between the second derivative of the phase shift δ_m and the the angle θ

$$\frac{d^2 \delta_m}{dm^2} - \frac{1}{2} \frac{d\theta}{dm} = 0. \quad (\text{E.5})$$

An analytical continuation in the complex m plane allows us to make the integral converge. Gaussian integration in Eq.(E.3) implies that

$$\left| \sum_m f_m(\theta) \right|^2 \approx \pi \left| \frac{dm}{d\theta} \right|, \quad (\text{E.6})$$

thus yielding the expected result:

$$\begin{aligned} \frac{1}{\tau} &\sim \frac{v_F}{k} \frac{1}{A} \int d\theta (1 - \cos \theta) \left| \frac{dm}{d\theta} \right| \\ &\sim \frac{v_F}{k} \frac{1}{A} \int dm \frac{\theta^2}{2} \sim \frac{v_F}{A} \int db \theta^2(b). \end{aligned} \quad (\text{E.7})$$

Appendix E: Semiclassical approximation

In this Section we present a tasteful derivation of the classical high energy limit for the relaxation time. The latter can be obtained by assuming classical diffusion along the geodesic trajectories across the bump and yields⁹:

$$\frac{1}{\tau} \approx \frac{v_F}{2A} \int db \theta^2(b). \quad (\text{E.1})$$

Here b is the impact parameter of the incoming particle, while θ is the scattering angle and A is the area of the sample. The starting point is the usual expression for the relaxation time of Eq.(III.15):

$$\frac{1}{\tau} = \frac{v_F}{kA} \int_0^\pi d\theta (1 - \cos \theta) \left| \sum_m f_m(\theta) \right|^2 \quad (\text{E.2})$$

given in terms of the scattering amplitudes $f_m(\theta) = [e^{i2\delta_m} - 1] e^{im\theta}$. At high energy, many m terms contribute to the sum, so that we take its continuum limit, which amounts to integrate over continuous values of the classical angular momentum $m = kb$. As forward scattering is excluded form Eq.(E.2), it is enough to apply the

In the last equality the conservation of the angular momentum $m = kb$ has been exploited, together with the remark that the scattering angle only depends on b in

the classical diffusion. This reproduces the desired high energy behavior.

The analysis of Eq.(III.15) provides a similar conclusion. The quantity $\delta_{m+1} - \delta_{m-1}$, appearing as the argument of the cosine, is $\approx 2 d\delta_m/dm$. At large incoming energies, $\delta_m \approx (2m+1)\pi/2$, which is consistent with the asymptotic form of the wavefunction given in Eq.(D.11). To lowest order we get, according to Eq.(E.4),

$$\sin^2 \delta_m - \cos(\delta_{m+1} - \delta_{m-1}) \sin \delta_{m+1} \sin \delta_{m-1} \approx \frac{\theta^2}{2}, \quad (\text{E.8})$$

so that we recover again

$$\frac{1}{\tau} \approx \frac{v_F}{kA} \int dm \frac{\theta^2}{2} \approx \frac{v_F}{A} \int db \theta(b)^2. \quad (\text{E.9})$$

-
- ¹ L. Fu, C. L. Kane, and E. J. Mele, Phys. Rev. Lett. **98**, 106803 (2007).
² L. Fu and C. L. Kane, Phys. Rev. B **76**, 045302 (2007).
³ J. E. Moore and L. Balents, Phys. Rev. B **121306**, 75 (2007).
⁴ M. Z. Hasan and C. L. Kane (2010), arXiv:1002.3895.
⁵ Y. Ran, Y. Zhang, and A. Vishwanath, Nature Phys. (2009).
⁶ J. C. Y. Teo and C. L. Kane, Phys. Rev. Lett. **104**, 046401 (2010).
⁷ J. C. Y. Teo and C. L. Kane, Phys. Rev. B **82**, 115120 (2010).
⁸ A. H. Castro Neto, F. Guinea, N. M. R. Peres, K. S. Novoselov, and A. K. Geim, Rev. Mod. Phys. **81**, 109 (2009).
⁹ J. P. Dahlhaus, C.-Y. Hou, A. R. Akhmerov, and C. W. J. Beenakker, Phys. Rev. B **82**, 085312 (2010).
¹⁰ M. Nakahara, *Geometry, Topology and Physics* (Adam Hilger, 1990).
¹¹ D.-H. Lee, Phys. Rev. Lett. **103**, 196804 (2009).
¹² A. Cortijo and M. A. H. Vozmediano, Nucl. Phys. B **763**, 293 (2007).
¹³ R. Egger, A. Zazunov, and A. L. Yeyati, Phys. Rev. Lett. **105**, 136403 (2010).
¹⁴ W.-Y. Shan, H.-Z. Lu, and S.-Q. Shen, New Journal of Physics **12**, 043048 (2010).
¹⁵ H. Zhang, C.-X. Liu, X.-L. Qi, X. Dai, Z. Fang, and S.-C. Zhang, Nature Phys. **5**, 438 (2009).
¹⁶ J. González, F. Guinea, and M. A. H. Vozmediano, Phys. Rev. Lett. **69**, 172 (1992).
¹⁷ F. de Juan, A. Cortijo, and M. A. H. Vozmediano, Phys. Rev. B **76**, 165409 (2007).
¹⁸ The carbon fullerenes admit a continuum description in terms of two Dirac equations on the surface of a sphere¹⁶. Lattice effects, such as scattering between the two equations, lead to corrections which scale as $(a/R)^2$, where a is the lattice spacing, see¹⁶. We do not find terms of similar magnitude at the surface of a topological insulator.
¹⁹ X.-Y. Feng, W.-Q. Chen, J.-H. Gao, Q.-H. Wang, and F.-C. Zhang, Phys. Rev. B **81**, 235411 (2010).
²⁰ R. Žitko, Phys. Rev. B **81**, 241414 (2010).
²¹ L. Landau and L. Lifshitz, *Quantum Mechanics Non-Relativistic Theory* (Butterworth-Heinemann, 1981).